INSTITUTE OF PHYSICS PUBLISHING SEMICONDUCTOR SCIENCE AND TECHNOLOGY

Semicond. Sci. Technol. **17** (2002) 1–10 PII: S0268-1242(02)24536-8

Physics of the formation of microdefects in dislocation-free monocrystals of float-zone silicon

V I Talanin, I E Talanin and D I Levinson

Zaporozhye State Engineering Academy, prosp. Lenina 226, 69006 Zaporozhye, Ukraine

E-mail: rio@zgia.zp.ua

Received 3 May 2001, in final form 19 November 2001
Published DD MMM 2002
Online at stacks.iop.org/SST/17/1

Abstract

We study non-doped dislocation-free monocrystals of float-zone silicon using transmission electronic microscopy, optical microscopy and x-ray topography. The crystals were obtained with various growth rates (1–9 mm min^{-1}) and were subjected to various kinds of thermal processing. We experimentally determine the temperatures at which microdefects of various types form, and we establish the mechanism of transformation of interstitial microdefects. On the basis of data in the literature and new results obtained by authors, we establish that the formation of microdefects in silicon occurs on two independent mechanisms: vacancy and interstitial. As a result of both these mechanisms, D-microdefects will be formed as interstitials agglomerate. We suggest that the critical parameter $V/G = C_{crit}$ describes the conditions of emerging (vanishing) vacancy microdefects. On the basis of these results, we suggest a physical model of the formation of microdefects in dislocation-free monocrystals of float-zone silicon, and we discuss other known models.

Q1

1. Introduction

During the production of dislocation-free monocrystals of silicon, it is necessary to solve the problem of their structural perfection. After the crystals are grown, structural microdefects form during cooling, which may include agglomerates of point defects (vacancies or silicon self-interstitial) and impurities. These structural defects can detrimentally affect the reliability of semiconducting devices and their performance. Since only high-purity silicon can be used in the modern electronic industry, it is necessary to have knowledge of the formation processes of defects in a semiconducting material [1, 2]. The systematic study of microdefects began in the 1960s, using methods of selective etching, decoration and x-ray topography [3–6]. On the basis of these studies, two types of microdefects were identified: A-microdefects (usually revealed as large etch-pits with smaller concentration) and B-microdefects (small etch-pits with higher concentration) [7–9]. Experience of crystal quenching [10] has shown that B-microdefects are formed first. With the help of transmission electronic microscopy (TEM) it was established that A-microdefects [11] and B-microdefects [12, 13] have an interstitial character. Typical A-microdefects are observed in stratified distribution at crystal growth rates of $V = 1$–3.5 mm min^{-1}, and in uniform distribution at $V < 1$ mm min^{-1}. B-microdefects are observed in stratified distribution at $V \leqslant 4.5$ mm min^{-1}. Such a distribution of microdefects reflects the distribution of their nucleation sites. During crystal growth, there is a fluctuation in the temperature due to the rotation of the crystal and a melt convection occurs [14]. Therefore, the microdefects grow, repeating crystal growth and stopping growth [14, 15]. The periodic modifications of the growth rate result in periodic modifications of the concentration of the impurities, in particular of carbon. Local maxima in the concentrations of A- and B-microdefects coincide with areas having a high concentration of phosphors [16]. As the heterogeneities of the distributions of phosphors and carbon are similar [17], we conclude that the formation of microdefects should include carbon atoms [11, 18]. Föll *et al* [18] have established that the concentration of microdefects increases with an increase of carbon content. Therefore, a stratified distribution of microdefects indicates the heterogeneous nature of their nucleation. Impurities such as oxygen (see, for example

Table 1. Microdefect classification in FZ Si.

Type	Physical nature	Size (nm)	V mm min^{-1}	Distribution in a plane (112)	N (cm^{-3})	References
A	Interstitial dislocation loops	up to 50 000	1–3.5	Stratified	$\sim 10^6$	[8–13, 15, 44]
B	Interstitial agglomerates of point defects	20–50	$\leqslant 4.5$	Stratified	$\sim 10^7$	[8–13, 15, 44]
C	Interstitial agglomerates of point defects	4–10	>4.5	Uniform	$\sim 10^{13}$	[13, 41, 44–46]
D	Interstitial agglomerates of point defects	4–10	>4.5	Uniform	$\sim 10^{13}$	[13, 41, 44–46]
I + V	Interstitial + vacancy	4–12	>6	Uniform	$\sim 10^{13}$	[13, 44, 45]

[19–30]) and carbon (see, for example [11, 17, 18, 31–39]), which are found in high concentrations in float-zone (FZ) silicon [40], have a direct effect on the formation of defects.

Further studies of monocrystals of silicon grown at high growth rates (more than 4.5 mm min^{-1}) have shown that these monocrystals contain uniformly distributed microdefects; this was revealed by selective etching as matt areas. Veselovskaya *et al* [41] observed these defects in FZ Si by selective etching and decoration techniques, and classified them as C- and D-microdefects depending on their distribution and concentration. Both these types of microdefects were found as areas of uniformly distributed defects with high densities. The difference between C- and D-defects is in the distribution of microdefects in these areas. D-microdefects are primarily concentrated as channels in a central part of the crystal whereas C-microdefects are revealed as rings or contours of an incorrect form. Later, Roksnoer *et al* [42], using x-ray topography followed by decoration with copper, suggested that D-microdefects have a vacancy characteristic in Czochralski-grown (CZ) silicon. However, in [12, 43] it has been shown that, for certain temperature conditions, the simultaneous formation of uniformly distributed interstitial microdefects of B-type and of uniformly distributed vacancies is possible. Using TEM, Sitnikova *et al* [13, 44–46] have investigated in detail the nature of D-microdefects in FZ Si, which were found in [41]. It was established that the D-microdefects (as well as the C-microdefects) formed the crystals that were obtained at growth rates of more than 4.5 mm min^{-1}, and have an interstitial nature. Furthermore, in the areas where no uniformly distributed D-defects were revealed by selective etching, vacancy microdefects which coexist together with interstitials microdefects were detected with TEM [44, 45]. These results are confirmed in a recent report by Bublik and Zotov [47]. They have revealed microdefects in silicon using x-ray diffuse scattering. They obtained results on defects which are formed in 'interstitial' and 'vacancy' modes of growth (these were interpreted as A-, B- and A′-defects). From these results, they concluded that all these defects are interstitial type. Furthermore, they detected other defects that had other signs of strain, i.e. vacancy type defects in the same areas of the crystal where the interstitial defects were observed. The results of [47] as well as the results of [13, 44–46] have also been confirmed by other recent research [48–52].

Thus, the results [42] cannot be represented as 'incorrect'. Since vacancy and interstitial microdefects coexist, the vacancy microdefects detected in [42] are not D-microdefects according to the classification [41]. The difference between the classifications in [41] and [42] are not basic, but they can cause disagreement in the determination of the types of microdefects. In this paper we use the classification of [41]. Table 1 shows the information from the literature about microdefect classification in FZ Si.

Defects which are identical to uniformly distributed D-defects in FZ Si are not observed in CZ Si. Thus, we think that the defects, similar to defects in FZ Si, which Roksnoer *et al* [42] called 'D-defects', should be in the areas of the crystal where the coexistence of interstitial and vacancy defects is revealed. As shown in table 1 we denote these areas by 'I + V'. In [42] CZ Si was studied, in which it is very difficult to reveal interstitial D-microdefects in comparison with FZ Si. However, we think that the processes of defect formation in both these types of crystal are identical [53, 54].

Thus, summarizing all the experimental results about the physical nature of microdefects in dislocation-free monocrystal FZ Si with a diameter of 30 mm, then using classification [41] it is possible to conclude that:

1. A-microdefects are interstitial dislocation loops with sizes of 1–50 μm with a Burgers vector of $\bar{b} = 1/2\,[110]$, which are in planes {111} and {110}.
2. B-microdefects are agglomerates of point defects of an interstitial type with sizes of 20–50 nm, some of which are in the plane {100}. Using TEM these are represented as rectangles and rhombs in the plane {111} with the parties on directions [110] and [100] respectively.
3. D-microdefects of an interstitial type are agglomerates of point defects with sizes of 4–10 nm. Considering these as small dislocation loops, it is possible to conclude that they can be in planes {100}, {110}, {111} and have of a Burgers vector of $\bar{b} = 1/2\,[100]$ and $\bar{b} = 1/2\,[110]$.
4. C-microdefects are completely identical to D-microdefects on TEM images, sign of deformation of crystalline lattice and their sizes.
5. It is suggested [44] that D-microdefects are uniformly distributed B-microdefects.
6. In crystals obtained at high growth rates (more than 6 mm min^{-1}) microdefects of vacancy type are formed simultaneously with microdefects of interstitial type in the same regions of the crystal.

Various theoretical models have been suggested to explain the regularities of microdefect formation in silicon. The main problems are the assumptions about the dominant type of point defects in crystals, their concentration, and the interaction between them. In some models [11, 15, 18, 55, 56] it was assumed that the dominating type of point defect in the crystal

is interstitial atoms of silicon. In other models [14, 57–60] it was supposed that the dominating type of defect is the vacancies. In contrast, Hu [61] and Sirtl [62] suggested the simultaneous independent coexistence of both main types of point defect at high temperatures. None of these models can explain the experimental results, which were obtained later using TEM, as shown De Kock [63].

According to the commonly accepted Voronkov theory [24, 64–66], the recombination rate between isolated vacancy and interstitial defects is high. Furthermore the diffusivity of interstitials is higher than the diffusivity of vacancies near the melting point. Finally the concentrations of vacancies is higher than the concentrations of interstitials at the melting point, where both concentrations are in thermal equilibrium. Only microdefects of either interstitial type (A- and B-microdefects, if the concentration of interstitial atoms is higher than the concentration of vacancies) or vacancy type (D-microdefects, if the concentration of vacancies is higher than the concentration of interstitial atoms) are formed in the crystal. According to [64], the type of dominating point defect depends on the parameter V/G (where V is the growth rate of the crystal and G is the axial temperature gradient); if $V/G < C_{\text{crit}}$, then interstitial atoms of silicon dominate in the crystal, if $V/G > C_{\text{crit}}$, then the vacancies dominate.

Thus, the sense of a Voronkov model consists of the following: (a) the existence of recombination between self-interstitials and vacancies for temperatures close to temperature of smelting; (b) the supposition of only the vacancy nature for primary grown-in microdefects and (c) independent areas of existence with only interstitial and vacancy microdefects.

However, these results, which are mainly theoretical conclusions that have not changed since 1982 [64], cannot explain some of the latest experimental results [13, 44–52]. Furthermore, the Voronkov theory does not take into account the influence of carbon in the formation of microdefects. The participation of carbon during defect formation results in a conclusion about the heterogeneous nature of the nucleation of microdefects [50, 51]. In the TEM studies reported in [45] it was established that equilibrium concentrations of vacancies and self-interstitials are approximately identical at temperatures close to the silicon melting point. Furthermore, the Voronkov theory does not explain the nature of 'defect-free'areas in silicon in which in [45] the microdefects of both types of a crystalline lattice strain were observed.

Therefore, the purpose of our paper is the development of an optimum physical model of formation, growth and transformation of microdefects in FZ silicon.

2. Experimental methods

Non-doped monocrystals of high resistivity (2200–4000 Ωcm) n-type silicon were grown using the float-zone technique in vacuum. The number of passes of a melting zone varied from 2 up to 10. The concentration of oxygen and carbon, determined by infrared (IR) absorption was less than 5×10^{15} cm^{-3}.

The crystals were received at a constant growth rate in the range 1–9 mm min^{-1}. Some crystals were obtained with a modification of growth rate on fixed length. Furthermore, in some cases the growth of the crystal was stopped for 30 or 60 min, and was resumed after that. To freeze-in the initial stages of microdefect formation we conducted crystal quenching. In order to study the reasons for the formation of microdefects the crystals were subjected to special thermal processing. Furthermore, to confirm the influence of oxygen on the formation of microdefects, experiments were conducted with intentional doping of crystals by oxygen. The oxygen doping was carried out from a gas phase when adding the steams of H_2O_2 to the growth chamber.

The method of selective etching of the crystal cross sections [64, 65] with subsequent TEM analyses was used to reveal the distribution of grown-in microdefects. The TEM studies were conducted by the analysis of diffractional images for case of peak contrast using the methods of Ashby–Brown and 2,5 D.

3. Results and discussion

3.1. Influence of quenching on a structure of monocrystals of silicon: determination of nucleation temperatures of microdefects of various types

The experiments with quenching of growing crystals allow us to freeze-in the earliest stages of defect formation. The quenching was conducted by decantation of a melting zone, which was blown out by a directed stream of argon. The characteristics of the distribution of microdefects and their types were determined after selective etching of longitudinal cuts of crystals on a plane (112), which is parallel to the growth direction [111]. These distributions are shown in figures 1 and 2. For A-microdefects, as shown in figures 1(*a*), 1(*b*) and 2(*a*), the formation temperature is equivalent $T_{\text{A}} \cong 1100$ °C. These figures also show that B-microdefects are formed at temperatures which are close to temperature of smelting (figure 2(*a*)). The studies of a surface texture of a separation show that the microdefects are not present at the front of crystallization. B-microdefects are formed immediately after the start of the cooling, due to the nucleation of complexes of interstitials atoms of silicon and atoms of impurities. Since the area which immediately adjoins the front of crystallization contains dislocations, it is very difficult to determine the beginning of the formation process of B-microdefects. Therefore, the best estimate of the nucleation temperature of B-microdefects that can be made from our data is ≈1380 °C. The distribution of D-microdefects, which is fixed by quenching, is shown in figures 1(*c*)–(*e*), 2(*b*) and 2(*c*). The formation temperature of the D-microdefects is $T_{\text{D}} \cong 1150$ °C. This temperature matches the temperature of dissociation of D-microdefects ($T = 1140$ °C), which was defined by Roksnoer [60]. Thus, this result confirms the determination of the formation temperature of D-microdefects. The temperature of the formation of interstitial D-microdefects (1150 °C) coincides with the temperature of dissociation of D-microdefects determined to be 1140 °C in [60, 69]. However, in [60, 69] the authors investigated CZ Si in which, according to [42], D-microdefects have a vacancy character. Therefore, if not to use a disputable nomenclature, in [60, 69] the temperature of interstitial microdefect formation

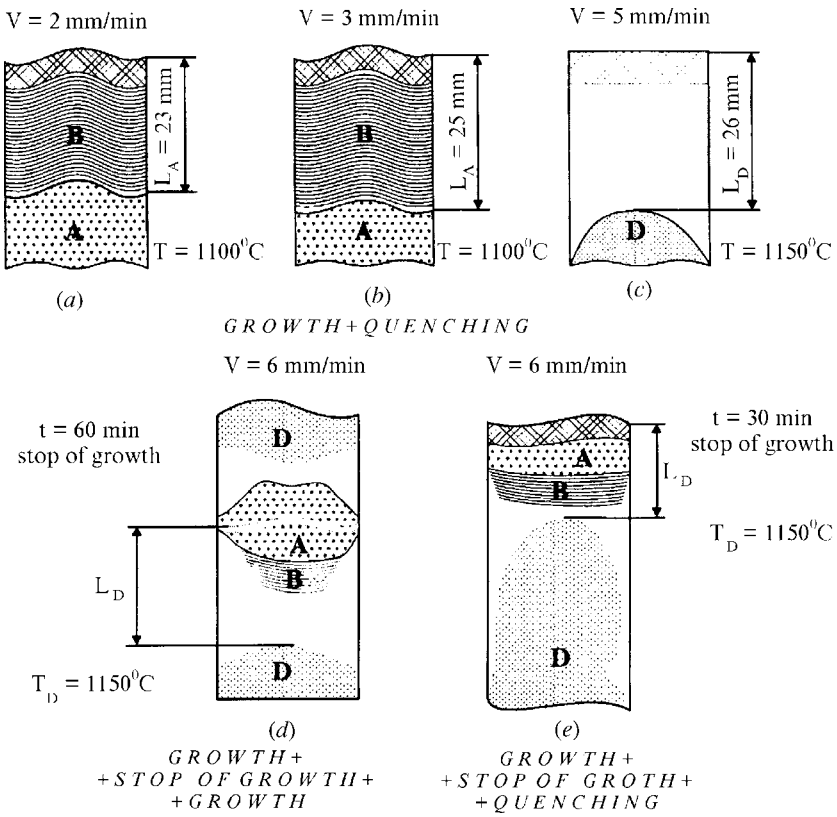

Figure 1. Schematic representation of distribution of microdefects at different growth rates after quenching and stop of growth.

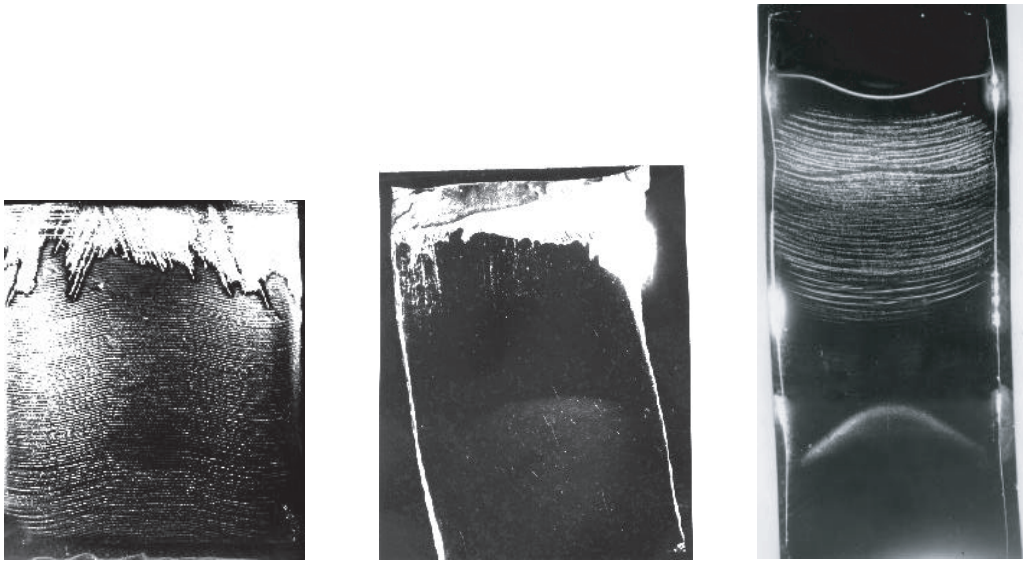

Figure 2. Distribution of microdefects at different growth rates after quenching and stop of growth (selective etching). (*a*) Distribution of A- and B-microdefects at $V = 3$ mm min^{-1} after quenching; (*b*) distribution of D-microdefects at $V = 5$ mm min^{-1} after quenching; (*c*) distribution of microdefects of various types at $V = 6$ mm min^{-1} after a stop of growth of crystal.

was established. This fact coincides well with our results from quenching experiments.

Furthermore, Neimark *et al* [70] measured thermal fields, which take place during the growth of monocrystals of silicon by the thermocouple. They suggested the following empirical formula to describe the dependence of an axial temperature gradient on the crystal growth rate

$$\frac{\mathrm{d}T}{\mathrm{d}L} = 10 + (L - 16)^2 \exp(-61.2V - 0.28) \qquad (1)$$

where L (cm) is the distance from the front of crystallization, and V (cm s^{-1}) is the crystal growth rate of crystal. The values calculated from equation (1) are shown in table 2.

3.2. Influence of high-temperature processing of crystals on the formation and transformation of microdefects

During production of semiconducting devices, the initial monocrystals of silicon are subjected to various thermal

Table 2. Formation temperatures of microdefects of various types.

Growth rate (mm min^{-1})	Condition of growth	Type of microdefects	Distance from the front of crystallization (mm)	Temperatures of formations (± 20 °C)
2	Quenching	A + B	23	$T_A = 1100$
3	Quenching	A + B	25	$T_B = 1380$
5	Quenching	D	26	$T_D = 1150$
6	Stop of growth $t = 60$ min	D	27	$T_D = 1150$
6	Stop of growth $t =$ 30 min + quenching	D	26	$T_D = 1150$

processings. As a result of these processings, the microdefects can be formed. It is supposed [44] that D-microdefects are an initial stage of the formation of interstitial defects, which are then transformed into B- and A-microdefects. Thus, it is important to determine how the process of the transformation of the initial grown-in D-microdefects occurs.

The experiments on thermal processing were conducted in two stages. In the first stage (I) the crystals obtained at $V =$ 6 mm min^{-1} with a growth stop of 60 min were investigated using selective etching and TEM. The same crystals were cut into four parts, each of which was then cut in half along the {112} planes. One half of each of the cut ingots was subjected to selective etching to reveal microdefects. The other half was subjected to thermal processing in vacuum for 60 min at the temperatures of 800, 900, 1000 and 1100 °C. In the second stage (II) the crystals, obtained at growth rates of 2, 3, 6 and 8 mm min^{-1}, were subjected to thermal processing (for 3 h) at the temperature of 1100 ± 20 °C in hydrogen atmosphere.

Stage I. The images of the distribution of microdefects in the crystal, which was obtained with a growth stop, are shown in figures 1(*d*) and 2(*c*). As is shown, there are all known types of microdefects in the crystal. This is confirmed using TEM. The appearance of microdefects is due to the thermal processing. The growth stop during some interval of time is a modification of the actual conditions of growth, i.e. the crystal during this interval receives additional processing. Furthermore, in these crystals below the positions of a growth stop of length $L_D = 27$ mm, a 'defect-free' area is formed, in which defects are not found by selective etching. For $L_D >$ 27 mm, there is an area with D-microdefects, which arise when $T \approx 1150$ °C.

We believe that the 'defect-free' area contains nucleation centres of microdefects (complexes nO$_i$). For each growth stop in the crystal oversaturation of self-interstitials I_{Si} occurs. These atoms interact with nO$_i$complexes. This process is stimulated by the catalytic role of carbon, which is in an item of substitution C_s:

$$(n\mathrm{O_i}) + \mathrm{I_{Si}} + \mathrm{C_s} \rightarrow \text{ B-microdefects.}$$

During the time which corresponds to the growth stop (for 60 min), these B-microdefects either transform into A-microdefects at $T \geqslant 1240 \pm 20$ °C, or remain as B-microdefects in the range of temperatures 1240–1190 °C.

Another 'defect-free' area arises in crystals obtained at $V = 5$ mm min^{-1}, between the front of the crystallization and the area with D-microdefects (see figures 1(*c*) and 2(*b*)). The 'defect-free' area contains very small defects of interstitial and vacancy types, as revealed by TEM and x-ray topography with subsequent copper decoration. The size of these defects is 3–7 nm and their density is $\approx 3.5 \times 10^4$ cm^{-2}, whereas in the area with D-microdefects the same defects have a size two times more and a density three times less ($\approx 1.2 \times 10^4$ cm^{-2}) than in the 'defect-free' area. Most likely, these defects are complexes of vacancies and interstitial atoms of oxygen O_i. These complexes are the predecessors of D-microdefects. It is possible that it is these complexes [VO_2] which were detected in silicon in radiation experiments [71, 72].

To confirm the influence of oxygen atoms on the formation of microdefects, a crystal was obtained at $V = 4$ mm min^{-1} with the simultaneous additional heating of a growing part. Usually B-microdefects will be formed at 4 mm min^{-1}, but in this case additional heating reduces the temperature gradient and a 'defect-free' area was formed at the centre of the crystal (figure 3(*a*)), i.e. the area containing vacancy and interstitial defects. After growth, the average part of the crystal was treated at $T = 1200$ °C for 20 min. This heat processing produces a rupture of the 'defect-free' channel and bands of B-microdefects are formed (figure 3(*b*)). Using IR absorption, it was found that, in an area of emerging B-microdefects, the concentration of carbon is 5×10^{16} cm^{-3}and that of oxygen is less, 2×10^{16} cm^{-3}. Thus, the experiment has confirmed the process of transformation of microdefects and the participation of carbon in the formation process of B-microdefects. After doping by oxygen from a gas phase, D-microdefects are formed and the concentration of B-microdefects is increased. After doping the concentration of B-microdefects is 2–6 $\times$ 10^5 cm^{-2} while before doping the concentration is 1–2 $\times$ 10^4 cm^{-2} (figure 3(*c*)).

To determine the influence of interstitial atoms of silicon on the formation of B- and A-microdefects, a crystal with a variable growth rate was obtained. The growth rate decreased by steps of $\Delta V = 0.5$ mm min^{-1} from $V = 3$ mm min^{-1} to $V = 0.5$ mm min^{-1} (figure 4). As shown in figure 4, at $V = 2$ mm min^{-1} large uniformly distributed A-microdefects are revealed, which are dislocation loops with sizes up to 20 μm. However, the stage change of the growth rate results in the formation of uniformly distributed 'clouds' of defects with sizes smaller than A-microdefects ($r_A = 70$–120 μm, $r_B = 10$–15 μm) and densities greater than A-microdefects $\left(N_A = 4 \times 10^2 \text{ cm}^{-2}, N_B = 1.3 \times 10^4 \text{ cm}^{-2}\right)$.

Our interpretation of this effect is as follows. The fluctuations of the growth rate result in an increasing concentration of interstitial atoms of silicon [73]. For a high concentration of interstitial atoms of silicon the size of the nuclei of microprecipitates of SiO_2 is increased [74]. But

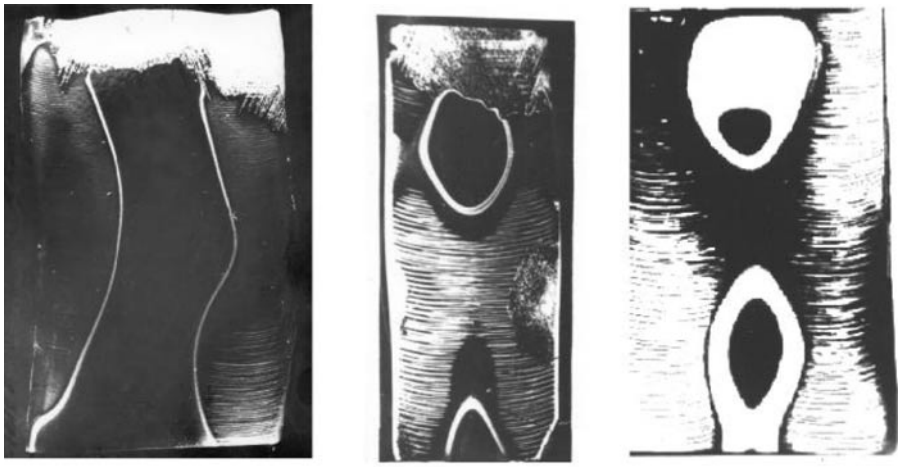

(*a*) (*b*) (*c*)

Figure 3. Distribution of the B- and D-microdefects after thermal processing (*a*) and (*b*), and oxygen doping (*c*).

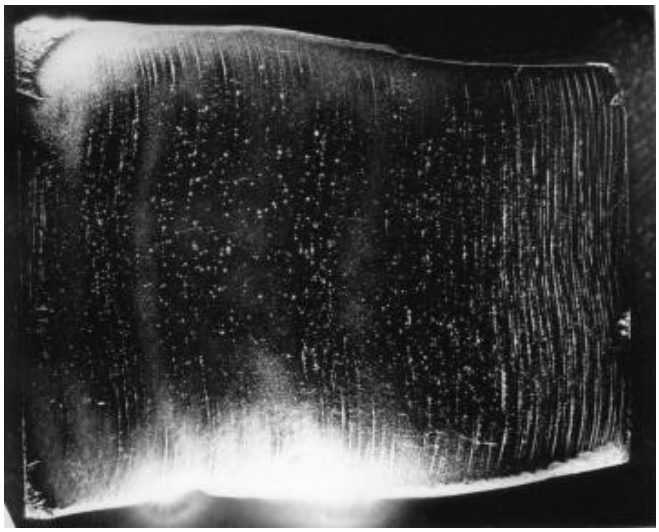

(*a*)

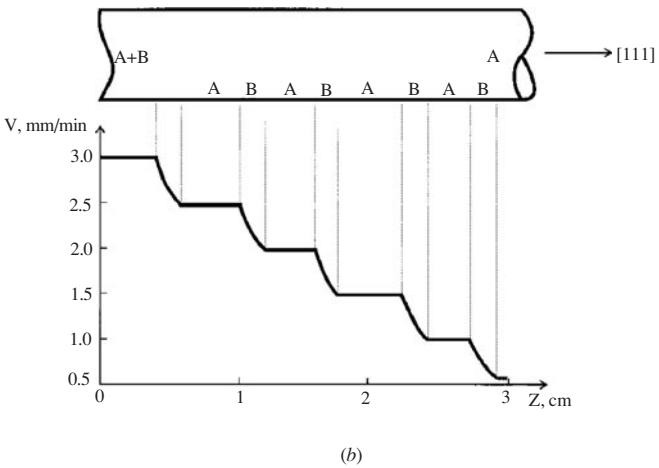

(*b*)

Figure 4. Distribution of microdefects in a crystal grown with a variable growth rate. (*a*) Distribution of microdefects (selective etching); (*b*) shematic image of distribution of microdefects (V denotes growth rate of crystal; Z denotes length of crystal and [111] denotes direction of growth).

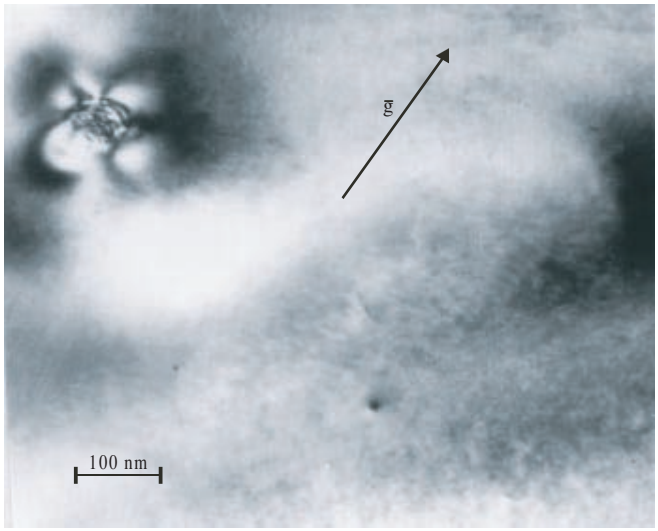

Figure 5. Defects as sockets in monocrystals of silicon after their thermal processing (dark field, $S > 0$, $\bar{g} = (2\bar{2}0)$).

at low growth rates the atoms C_s play a catalytic role in the formation of precipitation centres [75, 76]. Thus, the complexes will be formed which consist of atoms of carbon and interstitial atoms of silicon ($C_s + I_{Si} \leftrightarrow [C_s I_{Si}]$). As a result, B-microdefects will be formed in a uniform distribution.

In the case of thermal processing of crystals at 900 °C we observed an increase in the sizes of the D-microdefects up to 10–12 nm. Furthermore, in crystals processed at 1100 °C it was observed that defects such as sockets with sizes of 50–100 nm coexist with D-defects (figure 5). These defects are sources of dislocation loops of interstitial type. Completely identical defects (interpreted as B-microdefects) were revealed in crystals of silicon, which were obtained at $V = 3$ mm min^{-1} and were not subjected to thermal processing [15]. A TEM analysis of crystals obtained at $V = 3$ mm min^{-1} has shown that these defects are an intermediate stage of development between B- and A-microdefects.

Step II. In the second stage we investigated crystals which were obtained at different growth rates and thermally

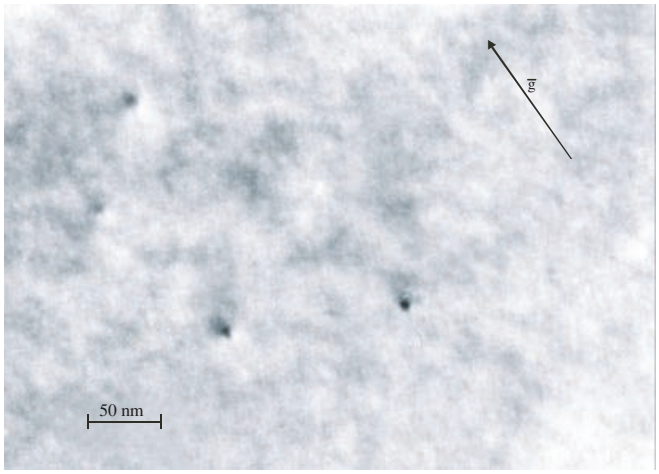

Figure 6. TEM-image of D-microdefects in crystals after their thermal processing (dark field, $S > 0$, $\bar{g} = (2\bar{2}0)$).

Table 3. Concentration of microdefects (cm^{-2}) in monocrystals of silicon after thermal processing.

	Growth rate (mm min^{-1})			
Type of defects	2	3	6	8
'Small' microdefects	1×10^6	1×10^6	2×10^6	1×10^6
'Large' microdefects	4×10^3	6×10^2	1×10^2	–
Dislocations	2×10^2	1×10^2	–	–

processed for 3 h. TEM revealed that the crystals before thermal processing contain microdefects of interstitial type (at $V < 6$ mm min^{-1}) and that interstitial and vacancy types coexisted (at $V > 6$ mm min^{-1}). In such crystals, in comparison with grown-in D-microdefects, the size of the defects increases up to 12–15 nm (we denote these defects as 'small' microdefects) (figure 6). Furthermore, the defects will be formed as sockets (see figure 5) or even more complicated types with sizes of 50–100 nm (we denote these defects as 'large' microdefects). The crystals obtained at $V \leqslant 3$ mm min^{-1} contain dislocations with a Burgers vector $\bar{b} = 1/2$ [100], which are in planes {111}. The experimental results are shown in table 3.

During thermal processing 'small' microdefects are generated, whereas the concentration of 'large' microdefects decreases with the increase of the growth rate. In crystals obtained at $V = 8$ mm min^{-1}, the interaction between vacancies and interstitials microdefects suppresses the formation of 'large' microdefects and dislocations.

Thus, the decrease of the growth rate and the additional thermal processing result in the growth and transformation of microdefects. On the basis of our experimental data it is possible to suggest the following mechanism of transformation of interstitial-type microdefects. We suppose that images of D-microdefects obtained by TEM can be considered as small dislocation loops. In this case they are in planes {111}, {100} and {110} [77]. With a decrease of the growth rate, we observe an increase in the size of interstitial D-microdefects (figure 7).

The fact that agglomerates are in planes {100} results in the generation of the interstitial atoms of silicon. The agglomerates of interstitial atoms promote the formation and

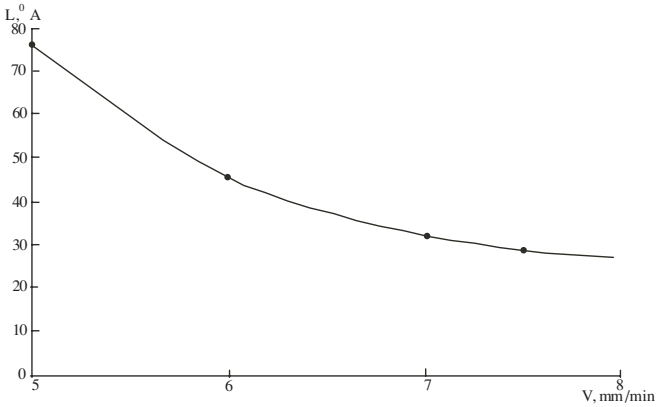

Figure 7. Experimental dependence a size of interstitial D-microdefects on the growth rate of crystal.

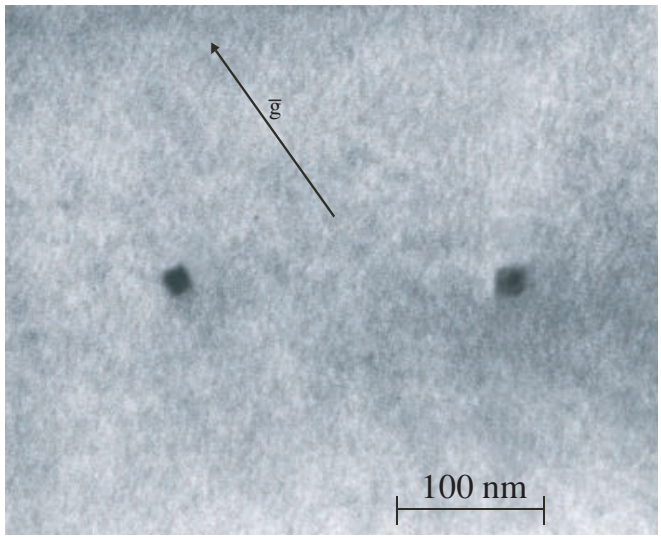

Figure 8. TEM-image of defects of the square and rhombic form (dark field, $S > 0$, $\bar{g} = (\bar{2}20)$).

growth of dislocation loops in planes {111}. Thus, D-microdefects, which are predecessors of B-microdefects, can exist in two forms: as flat congestions of point defects in planes {100} and as small dislocation loops in planes {111}. The TEM analysis of crystals with B-microdefects shows that some of them appear as rhombs and quadrates in a projection on a plane {111}. Such defects are in planes {100} (figure 8). The further growth of agglomerates in planes {100} results in the generation of dislocation loops in planes {110}. Such a process occurs at the expense of the mechanism of prismatic extrusion [78, 79]. As a result A-microdefects are formed as dislocation loops in planes {111} and {110} with a Burgers vector $\bar{b} = 1/2$ [110]. Therefore, the transformation of interstitial microdefects occurs according to following scheme: D-microdefects → B-microdefects → A-microdefects. During the transformation of interstitial microdefects with a decrease of the growth rate, the sizes of the defects are increased and their concentrations decrease (figure 9).

3.3. The mechanism of microdefect formation

With the help of TEM it is established that vacancy microdefects occur together with interstitial microdefects in

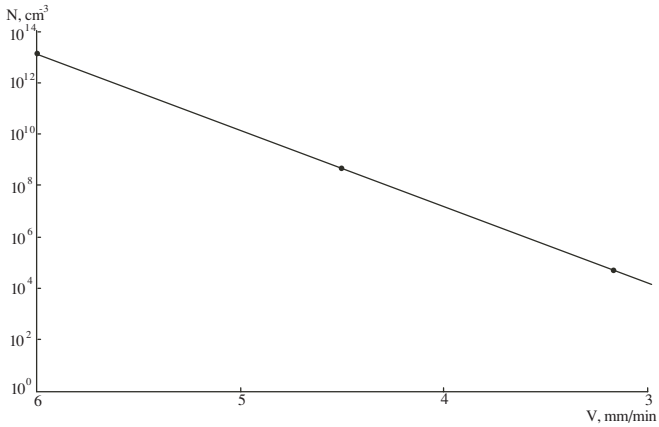

Figure 9. Experimental dependence of concentration of interstitial microdefects on the growth rate of crystal.

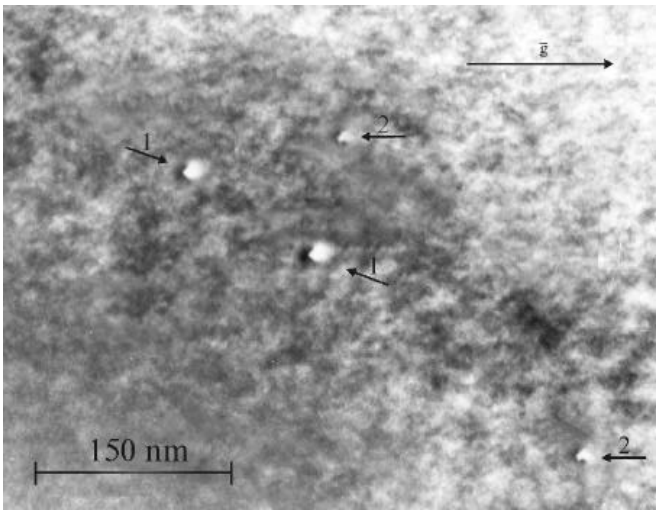

Figure 10. Defects of vacancy (1) and interstitial (2) type in crystal obtained at $V = 9$ mm min^{-1}, dark field, $\bar{g} = (\bar{2}20)$).

crystals grown at $V > 6$ mm min^{-1}; their concentration increases with the increasing crystal growth rate [44]. The ratio of vacancy and interstitial microdefects in samples obtained at $V = 7.5$ mm min^{-1} is approximately 1:4. In crystals obtained at $V = 9$ mm min^{-1}, interstitial and vacancy defects coexist approximately in identical concentrations (figure 10). Thus, the critical crystal growth rate, for which vacancy microdefects occur, is in the range of $6 < V < 6.5$ mm min^{-1} (figure 11).

With the help of TEM it is also established that the concentrations of native point defects near the front of the crystallization are approximately identical [45]. Thus, over-saturated solid solutions of native point defects will be formed during cooling in the bulk of the crystal which eventually breaks up; therefore the microdefects will be formed. The impurities of carbon and oxygen facilitate the nucleation process of microdefects. In the Voronkov theory it is suggested that, in the initial stage of disintegration of oversaturated solid solutions of point defects, the main process is recombination between vacancies and interstitial atoms of silicon. However, in [62, 80, 81] it was supposed that the direct recombination between vacancies and interstitial atoms of silicon is hampered, which is stipulated by the existence of an energy barrier. Tempelhoff [12, 43] argued that the

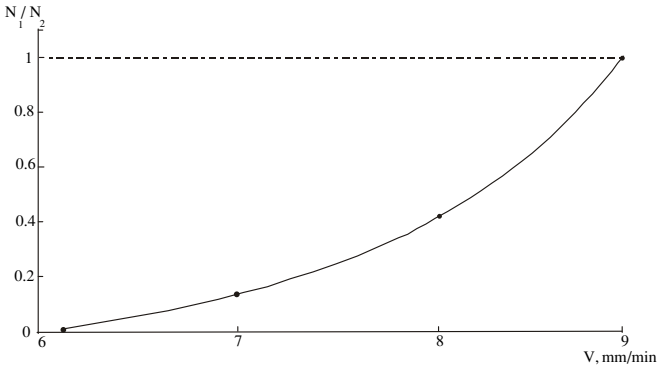

Figure 11. Experimental dependence of the ratio of concentration of vacancy (N_1) and interstitial (N_2) microdefects on growth rate of crystal.

recombination takes place only on some centres (B- and A-microdefects, dislocations, surface of crystal), and that direct recombination is impossible. The same problem was treated in detail in [82–88], where it was shown that point defects in silicon (vacancies and self-interstitial) have an extended characteristic at very high temperatures, i.e. one atom (or one vacancy) 'are extended' on some nuclear volumes. According to this model the recombination occurs only for 'simultaneous compression from both these defects in a neighbourhood of one nuclear volume' [89]. It was concluded from this observation [89] that the recombination of point defects in an initial stage of their interaction at high temperatures is hindered by an activation barrier, which includes enthalpy and entropy components. The main contribution introduces an entropy component, reaching a value of 11–11.5 K [89]. The barrier is decreased if the temperature is lowered and disappears at low temperatures. Thus, the disintegration of over-saturated solid solutions of native point defects proceeds simultaneously on two mechanisms: vacancy and interstitial [52, 90].

For the vacancy mechanism, theoretically only vacancy aggregation and joint vacancy–impurity aggregation are possible [64]. Vacancy–impurity aggregation begins earlier than a vacancy aggregation. Interstitial atoms of oxygen are very mobile, and therefore the formation of complexes is simulated by leaving interstitial oxygen in positions of substitution O_s

$$O_i + V_{Si} \rightarrow O_s \rightarrow 2O_s + 3O_s + \cdot + nO_s.$$

At lower temperatures, O_s can be formation centres of microprecipitates of oxygen. When microprecipitates are formed, there is a surplus of volume and one vacancy will be consumed by a growing precipitate for each two oxygen atoms precipitated. The absorption of vacancies and impurities by growing microdefects results in a decreased concentration of vacancies in comparison with oxygen concentration. As a result, precipitates begin to absorb oxygen without participation of vacancies, their sizes are increased, and then the type of strain around them varies from vacancy (tensile) to interstitial (compressive). The full transition boundary can be determined from the relation V/G. Thus, the parameter C_{crit} of the theory [64] does not describe a condition of mode change of growth (interstitial or vacancy). This parameter describes conditions of the vanishing (emerging) of microdefects of a

vacancy type, as a result of diffusion and interaction of point defects during the cooling of the crystal.

The centres of nucleation in a base of interstitial atoms of oxygen exist also for the interstitial mechanism. However, here a catalytic role is played by carbon atoms. The over-saturation of interstitial atoms of silicon results in the appearance of complexes $[C_sI_{Si}]$

$$C_s + I_{Si} \leftrightarrow [C_sI_{Si}].$$

The decrease of the critical radius $[C_sI_{Si}]$ nuclei and the acceleration of a diffusion C_s occur here. Thus, agglomerates $[C_sI_{Si}]$ are formed. Furthermore, during supersaturation of I_{Si} co-precipitation of O_i and C_s can occur [23, 35, 91]. Thus, for the formation of B-microdefects

$$I_{Si} + C_s \rightarrow [CI] + O_i \rightarrow \text{B-microdefects}.$$

The growth of interstitial microdefects results in a significant decrease of the concentration of interstitial atoms of silicon. It creates conditions for precipitations of impurities. In this case the formation of particles of impurity phase is accompanied by the generation of self-interstitial atoms in positions between knots of the lattice. Thus, two types of interstitial microdefects are formed: as interstitial congestion (drains for interstitial atoms of silicon) and as impurity precipitates (sources of these atoms).

Both mechanisms (vacancy and interstitial) result in the formation of small interstitial agglomerations, i.e. D-microdefects. These agglomerates are uniformly distributed small B-microdefects. These mechanisms are described by the following equations:
For the vacancy mechanism:

(1) $nO_i + V_{Si} \rightarrow n(VO_2) \rightarrow$ vacancy microdefects.
(2) $n(VO_2) + O_i + \cdot + nO_i \rightarrow n[(V_mO_n) + I_{Si}] \rightarrow$ D-microdefects.

For the interstitial mechanism:

(1) $C_s + I_{Si} \rightarrow (C_sI_{Si}) \rightarrow$ D-microdefects.
(2) $(CI) + O_i \rightarrow n[(C_sI_{Si}) + O_i] \rightarrow$ B-microdefects.
(3) B-microdefects + $I_{Si} \rightarrow$ A-microdefects.

Furthermore, in [44, 46] TEM has revealed two types of image of D-microdefects: as agglomerates of atoms with a crystalline structure and as agglomerates of atoms with an amorphous structure. In [46] it was shown that such images give microprecipitates of the amorphous phases of SiO_2. From our point of view the crystalline phases give the precipitates SiC [53]. Both types of D-microdefects are defects of an interstitial type. These data also confirm the existence of two mechanisms of microdefect formation.

4. Conclusions

Thus, the formation of vacancy and interstitial microdefects is due to the disintegration of the over-saturated solid solution of native point defects. All known types of microdefects are formed as a result of the interaction of native point defects with impurities of oxygen and carbon. The concentrations of vacancies and interstitial atoms of silicon are approximately identical near to the front of crystallization. The recombination between them in an initial stage of their interaction at high temperatures is hampered. Therefore, the formation of microdefects occurs simultaneously on two mechanisms: vacancy and interstitial. Vacancy and interstitial microdefects coexist in crystals. The parameter $V/G = C_{crit}$ describes the emerging (vanishing) conditions of vacancy microdefects in crystals.

The experiments of quenching of crystals have enabled us to investigate the initial stages of defect formation and to determine the temperatures at which the formation of microdefects of various types is possible. The thermal processing of the crystals results in the transformation of one type of microdefect to another. The obtained results show that microdefects (agglomerates of point defects and atoms of impurities) are present even in dislocation-free monocrystals of silicon after growth. The thermal processing promotes the 'improvement' of such agglomerates due to the effect of internal gettering of impurities on the nucleation centres of the microdefects. Thus, thermal processing plays an important role in the manufacture of perfect silicon crystals.

Acknowledgment

The authors are very grateful to the Board of Zaporozhye Titan-Magnesium Plant for providing the possibility of using of the necessary equipment and for help in deriving the crystals.

References

[1] Gatos H C 1990 *Defect Control in Semiconductors* vol 1 (Amsterdam: Elsevier) p 3
[2] Abe T 1993 *JAERI-M* **92** 7
[3] Plaskett T S 1965 *Trans. Met. Soc. AIME* **233** 809
[4] Abe T, Samizo T and Maruyama S 1966 *Japan. J. Appl. Phys.* **5** 255
[5] Hattori H and Kato N 1966 *J. Phys. Soc. Japan* **21** 1773
[6] Chikawa J, Asada Y and Fujimoto I 1970 *J. Appl. Phys.* **41** 1922
[7] De Kock A J R 1970 *Appl. Phys. Lett.* **16** 100
[8] De Kock A J R 1971 *J. Electrochem. Soc.* **118** 1851
[9] De Kock A J R 1973 *Philips Res. Rep.* **1** 1
[10] De Kock A J R, Roksnoer P J and Boonen P G T 1974 *J. Cryst. Growth* **22** 311
[11] Föll H and Kolbesen B O 1975 *J. Appl. Phys.* **8** 319
[12] Tempelhoff K and Van Sung N 1982 *Phys. Status Solidi* A **70** 441
[13] Sitnikova A A *et al* 1984 *Phys. Status Solidi* A **81** 433 **Q2**
[14] Abe T, Harada H and Chikawa J 1983 *Physica* B/C **116** 139
[15] Petroff P M and De Kock A J R 1975 *J. Cryst. Growth* **30** 117
[16] Kamm J B and Müller R 1977 *Solid State Electron.* **20** 105
[17] Abe T, Abe Y and Chikawa J 1973 *Semiconductor Silicon* (Princeton, NJ: Electrochemical Society) p 95
[18] Föll H, Gösele U and Kolbesen B O 1977 *J. Cryst. Growth* **40** 90
[19] Patel J R 1977 *Semiconductor Silicon* (Pennington, NY: Electrochemical Society) p 521
[20] Carlberg T, King T B and Witt A F 1981 *J. Electrochem. Soc.* **127** 129
[21] Patel J R 1981 *Semiconductor Silicon* (Princeton, NJ: Electrochemical Society) p 139
[22] Bourret A, Thibalt -Desseaux J and Seidman D N 1984 *J. Appl. Phys.* **55** 825

[23] Bourret A 1985 *Proc. 13th Int. Conf. Defects in Semiconductors 1984 (Coronado)* p 129
[24] Voronkov V V and Milvidskii M G 1988 *Kristallografiya* **33** 471 (in Russian)
[25] Chadi D J 1990 *Phys. Rev.* B **41** 10 595
[26] Gall P *et al* 1990 *Defect Control in Semiconductors* vol 1 (Amsterdam: Elsevier) p 255
[27] Puzanov N I and Eidenzon A M 1992 *Semicond. Sci. Technol.* **7** 406
[28] Ikari A *et al* 1994 *Japan. J. Appl. Phys.* **33** 1723
[29] Borghesi A, Pivac B, Sassella A and Stella A 1995 *J. Appl. Phys.* **38** 4169
[30] Umeno S *et al* 1999 *Japan. J. Appl. Phys.* **38** 5725
[31] Nozaki T, Yatsurugi Y and Akiyama N 1970 *J. Electrochem. Soc.* **117** 1566
[32] Matlock J H 1977 *Semiconductor Silicon* (Pennington, NY: Electrochemical Society) p 32
[33] Matsushita Y, Kishino S and Kanamori M 1980 *Japan. J. Appl. Phys.* **19** L101
[34] Kolbesen B O and Mühbaur A 1982 *Solid State Electron.* **15** 759
[35] Benton K L, Oates A S and Livingston F M 1983 *J. Phys. C: Solid State Phys.* **16** 1667
[36] Shimura F, Hockett R S and Reed D A 1985 *Appl. Phys. Lett.* **46** 941
[37] Drevinsky P J, Caefer C E, Kimerling L C and Benton J L 1990 *Defect Control in Semiconductors* vol 1 (Amsterdam: Elsevier) p 341
[38] Gupta S *et al* 1992 *Semicond. Sci. Technol.* **7** 5
[39] Ueki T, Itsumi M and Takeda T 1999 *Japan. J. Appl. Phys.* **38** 5695
[40] Gorshkov V G *et al Phys. Status Solidi* **A 106** 363
[41] Veselovskaya N V, Sheikhet E G, Neimark K N and Falkevich E S 1977 *Rost i legirovanie poluprovodnikovykh kristallov i plenok* part 2 (Novosibirsk: Nauka) p 284 (in Russian)
[42] Roksnoer P J and Van Den Boom H M B 1981 *J. Cryst. Growth* **53** 563
[43] Tempelhoff K and Van Sung N 1982 *Phys. Status Solidi* A **72** 617
[44] Sitnikova A A *et al* 1985 *Phys. Status Solidi* A **90** K31
[45] Sitnikova A A *et al* 1986 *Fizika Tverdogo Tela* **28** 1829 (in Russian)
[46] Sitnikova A A, Sorokin L M and Sheikhet E G 1987 *Fizika Tverdogo Tela* **29** 2623 (in Russian)
[47] Bublik V T and Zotov N M 1997 *Cryst. Rep.* **42** 1033
[48] Nango N, Iida S and Ogawa T 1999 *J. Appl. Phys.* **38** 5695
[49] Iida S *et al* 1998 *Japan. J. Appl. Phys.* **37** 241
[50] Iida S *et al* 2000 *Japan. J. Appl. Phys.* **39** 6130
[51] Kim Y K, Ha Tae S and Yoon J K 1988 *J. Mater. Sci.* **33** 4627
[52] Talanin V I 2000 *Siberian Russian Workshops and Tutorials on Electron Devices and Materials (EDM'2000). Proc. NSTU (Novosibirsk)* p 87
[53] Talanin V I, Talanin I E and Levinson D I 2001 *Single Crystal Growth and Heat and Mass Transfer. Proc. SSC RF IPPE (Obninsk)* vol 1 p 205
[54] Talanin V I, Talanin I E and Levinson D I 2001 *Abstracts of ICDC-01 (Giessen)* p 113
[55] De Kock A J R 1977 *Semiconductor Silicon* (Pennington, NY: Electrochemical Society) p 508
[56] Tan T Y and Gösele U 1985 *Appl. Phys.* A **37** 1
[57] Chikawa J and Shirai S 1977 *J. Cryst. Growth* **39** 328
[58] Chikawa J and Shirai S 1979 *Japan. J. Appl. Phys.* **18** 153
[59] Van Vechten J A 1978 *Phys. Rev.* B **17** 3197
[60] Roksnoer P J 1984 *J. Cryst. Growth* **58** 596
[61] Hu S M 1977 *J. Vac. Sci. Technol.* **14** 17
[62] Sirtl E 1977 *Semiconductor Silicon* (Pennington, NY: Electrochemical Society) p 4
[63] De Kock A J R 1981 *Defect in Semicond.* (Amsterdam: North-Holland) p 309
[64] Voronkov V V 1982 *J. Cryst. Growth* **59** 625
[65] Voronkov V V, Falster R and Holzer J C 1997 *Cryst. Defects and Contamination: Ttheir Impact and Control in Device Manufacturing II*. (Pennington, NY: Electrochemical Society) p 3
[66] Voronkov V V and Falster R 1998 *J. Cryst. Growth* **194** 76
[67] Sirtl E and Adler A 1961 *Z. Metalkunde* **52** 529
[68] Secco d'Arogona F 1972 *J. Electrochem. Soc.* **119** 948
[69] Wijaranakula W and Chiou H D 1994 *Appl. Phys. Lett* **64** 1030
[70] Neimark K N, Sakharov B A, Chulitsky V F and Osovsky M I 1970 *Metallurgiya (Moscow) Kremnii i Germanii* **2** p 32 (in Russian)
[71] Lindström J L and Svensson B G 1985 *Mater. Res. Soc. Symp. Proc.* **59** 45
[72] Londos C A, Sarlis N, Fytros L G and Papasterqiou K 1996 *Phys. Rev.* B **53** 6900
[73] Puzanov N I and Eidenzon A M 1996 *Cryst. Rep.* **41** 134
[74] Tan T Y and Kung C Y 1986 *J. Appl. Phys.* **59** 917
[75] Kishino S, Matsushita Y, Kanamori M and Iizuka T 1982 *Japan. J. Appl. Phys.* **21** 1
[76] Gösele U 1986 *Mat. Res. Soc. Symp. Proc.* **59** 419
[77] Talanin V I, Talanin I E and Levinson D I 2001 *Abstracts of ICCG-13 (Kyoto)* p 32
[78] Tan T Y and Tice W K 1976 *Phil. Mag.* **34** 615
[79] Taylor W J, Gösele U and Tan T Y 1992 *J. Appl. Phys.* **72** 2192
[80] Fair R B 1980 *J. Appl. Phys.* **51** 5828
[81] Antoniadis D A and Moskowitz I 1982 *J. Appl. Phys.* **53** 6788
[82] Seeger A and Chik K P 1968 *Phys. Status Solidi* **29** 455
[83] Seeger A 1971 *Radiat. Eff.* **9** 15
[84] Seeger A and Frank W 1972 Radiation damage and defects in semiconductors *Inst. Phys. Conf. Ser. (London and Bristol)* **16** p 262
[85] Seeger A, Föll H and Frank W 1976 Radiation effects in semiconductors, *Inst. Phys. Conf. Ser. (London and Bristol)* **31** p 12
[86] Gösele U, Frank W and Seeger A 1980 *J. Appl. Phys.* **23** 361
[87] Gösele U, Morehead F, Frank W and Seeger A 1981 *Appl. Phys. Lett.* **38** 157
[88] Stolwijk N A *et al* 1987 *Phys. Status Solidi* A **104** 225
[89] Gösele U, Frank W and Seeger A 1983 *Solid State Commun.* **45** 31
[90] Talanin I E, Talanin V I and Levinson D I 2000 *Abstracts of NCCG-9* (RAS Moscow: Inst. Cryst.) p 216 (in Russian)
[91] Shimura F, Hockett R S, Reed D A and Wayne D N 1985 *Appl. Phys. Lett.* **47** 794